Autonomous Ship Deck Landing of a Quadrotor Using Invariant Ellipsoid Method

CHUN KIAT TAN
JIANLIANG WANG, Senior Member, IEEE
Nanyang Technological University
Singapore

YEW CHAI PAW
DSO National Laboratories
Singapore

FANG LIAO
National University of Singapore
Singapore

This paper proposes an invariant ellipsoid-based method for the controller design and gain synthesis of a low-cost quadrotor autonomous ship deck landing system subjected to wind disturbance and measurement noise. This method optimizes the quadrotor performance, hence achieving soft landing. A complete control architecture for the quadrotor is also presented. Simulations are performed using a realistic ship deck model in the presence of measurement noise and wind disturbance with a quadrotor.

Manuscript received November 11, 2014; revised July 3, 2015; released for publication January 19, 2016.

DOI. No. 10.1109/TAES.2015.140850.

Refereeing of this contribution was handled by L. Rodrigues.

Authors' addresses: C. K. Tan, J. Wang, Nanyang Technological University, School of Electrical and Electronic Engineering, 50 Nanyang Avenue, Singapore, 639798 Singapore; Y. C. Paw, DSO (Marina Hill) 11 Stockport Road, Singapore, 117605; F. Liao, Temasek laboratories, National University of Singapore, T-Lab Building, 5A, Engineering Drive 1, Singapore 117411. Corresponding author is J. Wang, E-mail: (ejlwang@ntu.edu.sg).

I. INTRODUCTION

The use of an unmanned aerial vehicle (UAV) in open seas has provided both military and civilian operators with the capability to conduct efficiently reconnaissance and survey on the vast ocean. These operations often require the UAV to take off and land on a ship or a vessel, typically in rough seas. Furthermore, developments in vertical takeoff and landing (VTOL) UAV, especially quadrotors, reduce the cost and allow for an easier and safer deployment, thus leading to increasing interests in using quadrotors onboard ships.

However, it is challenging to perform autonomous landing of a quadrotor on a ship deck because ship-wave interactions result in pseudorandom ship motion that increases the difficulty of autonomous landing. During landing, the quadrotor needs to take into account the relative velocity and distance between itself and the ship in order to achieve a safe landing. Soft landing is achieved by reducing the relative speed between the quadrotor and the ship. Erratic ship motion and high impact velocity can cause collisions and result in damage to the quadrotor and/or the ship.

Autonomous landing control primarily consists of two main parts: data acquisition and control execution. Data acquisition is the measurement or estimation of quadrotor position relative to the ship using either onboard sensors or ship-borne sensors. On the other hand, control execution refers to the control algorithm that transforms the measurement input into the control actuation of the quadrotor. It dictates how the quadrotor reacts to the changes in environment and ship motion that is critical for a soft landing.

Traditionally, onboard relative position measurement is replaced by a ship motion predictor; ship motion prediction techniques are used to provide the quadrotor with a prediction of the ship motion. The quadrotor then reacts to this prediction by generating a trajectory for soft landing. For instance, Avanzini et al. [1] develop both online and offline trajectory generators and tracking algorithm based on ship motion prediction for a VTOL UAV to keep it at a certain prescribed height above the ship deck. Marconi et al. [2], on the other hand, use an internal model approach to account for the ship deck oscillation while maintaining a constant clearance. Furthermore, Yang et al. [3, 4] use an autoregressive exogenous model and a Prony analysis approach to estimate ship motion. However, Yang et al. [3] note that the ship motion predictor is unable to provide long-term accurate prediction and also requires substantial time to initialize. This motivates the use of a ship motion prediction-free control approach that is not limited by the accuracy of the ship motion predictor.

Recent advances in sensor technology has reduced the dependency on ship motion predictor because relative position between the quadrotor and the ship are increasingly accurately measured in real time. This allows control algorithms to react almost instantaneously to the

measured information and achieve soft landing on a randomly moving platform like a ship. Range sensors such as radar or lidar [5, 6] are commonly used to provide the quadrotor with reliable relative motion information. In addition, in recent years, vision-based control is also gaining popularity and is used in ship deck landing operations [7–9]. Vision-based sensors are used to provide the flight controller with an estimate of the quadrotor position relative to the ship and control actions are executed accordingly. However, vision-based sensors are heavily affected by weather and visibility, and thus should not be relied upon fully for landing operation, especially during adverse conditions. Infrared sensor is sometimes used [10] to complement vision sensor.

The accuracy achieved by these measurement techniques allows the implementation of simpler and less complex control structures. This simplification in control structure is largely beneficial to the development of modern low-cost VTOL UAVs such as the quadrotor that are smaller in size and possess less computational power. For instance, the quality of the relative position measurement provided by the vision sensors developed by Venugopalan et al. [11] and Ling et al. [12] allows for the implementation of a proportional integral derivative (PID) landing control law for their quadrotors. Furthermore, other linear techniques such as linear quadratic integral, model predictive control, and loop-shaping design that are applied to UAV ship deck landing are analyzed and compared by Sandino et al. [13]. In particular, PID control is used by [5, 11, 12, 14, 15] in autonomous ship deck landing application and is also widely used by quadrotors due to its easy implementation and low computational cost.

This work is motivated by the computational cost and implementation advantage of using linear control techniques such as PID control and state feedback control as compared to ship motion predictor-based controls that is made possible by the advances in sensing technology. In these control techniques, the controller gains are carefully tuned according to certain performance measures. In ship deck landing, a critical performance measure is the response of the system under disturbances such as ship motion and wind. These disturbances act persistently on the closed-loop system, and a good controller must be able to minimize their effects on the UAV. In particular, the relative speed between the UAV and the ship deck must be as close to zero as possible in the presence of pseudorandom ship motion to achieve a soft landing.

A review of the work on linear control designs shows that persistent disturbances are often not explicitly considered in the gain optimization routine. For instance, the linear quadratic regulator and model predictive controllers studied by Sandino et al. [13] and Ngo and Sultan [16] are optimal with respect to objective functions of specific forms and do not consider the pseudorandom ship motion explicitly. Furthermore, the more commonly used PID controller [5, 11, 12, 14, 15], which is a kind of state feedback control, is usually tuned such that the settling time or maximum overshoot is minimized. Performance measures with respect to disturbances such as ship motion are often not explicitly considered.

However, in the work of Tan and Wang [15, 17], the effects of persistent disturbance is evaluated in terms of a minimum invariant ellipsoid for the state feedback and PID controller. The minimum invariant ellipsoid is the smallest ellipsoid that bounds the state response of a system subjected to persistent bounded disturbance. A small minimum invariant ellipsoid indicates good closed-loop performance with respect to the external disturbance. This approach, also known as the invariant ellipsoid method, is based on the general theory developed in [18–20]. Other than autonomous ship deck landing of UAVs, invariant ellipsoid method is also applied in other situations such as spacecraft stabilization [21] and sliding mode control [22]. Extensions to this method are developed in [23–25].

Invariant ellipsoid method is well-suited for the application in UAV ship deck landing due to its quantitative measurement of the effects from the ship motion. However, the vertical landing of a quadrotor on a ship deck is also subjected to measurement noise and wind disturbances. Their effects are not considered by Tan and Wang [15, 17]; therefore, this motivates the work in this paper to formulate a controller gain optimization problem that considers explicitly the effects of multiple persistent disturbances such as ship motion, wind disturbance, and measurement noise using an invariant ellipsoid method.

The key contribution of this paper is the generalization of the invariant ellipsoid condition proposed in [15, 17] that allows the computation of a worst-case bound on the state response for a linear system subjected to multiple bounded disturbances. An optimization problem that solves for the optimal control gain under these disturbances is also presented. Although ship heave motion, wind disturbances, and measurement noise are the disturbances considered in this paper, the approach proposed in this paper can be generalized to include other disturbances. In addition, this paper also highlights some of the properties of the proposed approach that include preserved optimality, exponential attraction to the invariant ellipsoid, and response to stochastic disturbance. Thereafter, an extension of the proposed approach to include treatment for measurement noise is also given.

This paper is organized in the following way. Section II provides the dynamic model of the quadrotor. Section III decouples the problem into separate altitude and lateral control and gives the details of the altitude controller based on the invariant ellipsoid method for multiple disturbances. Section IV presents simulation results and discussions followed by some concluding remarks in Section V.

II. DYNAMIC MODEL OF QUADROTOR

Kinematic and dynamic equations of quadrotors are discussed in detail in [26, 27], and the dynamic model is adopted in this paper and reproduced as discussed below.

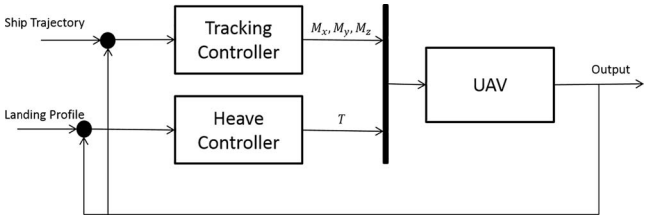

Fig. 1. Block diagram of overall control structure.

A. Translational Kinematics and Dynamics

The position and velocity of the quadrotor is described in an inertial reference frame,

$$\dot{p}^{(i)} = v^{(i)}, \tag{1}$$

where $p^{(i)}$ and $v^{(i)}$ are the position and velocity of the quadrotor in the inertial reference frame, respectively. The dynamic equation of the quadrotor is given as

$$m\dot{v}^{(i)} = -R_{bi}^T T\hat{e}_3 + mg\hat{e}_3, \tag{2}$$

where m is the mass of the quadrotor, g is the gravitational acceleration, $\hat{e}_3$ is the unit vector in the z axis (vertical downward), and R_{bi} is the rotation matrix from the body reference frame to the inertial reference frame. In this equation, we have assumed minor forces acting on the quadrotor such as the aerodynamic forces to be insignificant.

B. Rotational Kinematics and Dynamics

The quaternions allow a singularity-free description of the quadrotor attitude. The kinematic equation is given as [28]

$$\begin{pmatrix} \dot{\phi} \\ \dot{\theta} \\ \dot{\psi} \end{pmatrix} = \begin{pmatrix} 1 & \tan\theta\sin\phi & \tan\theta\cos\phi \\ 0 & \cos\phi & -\sin\phi \\ 0 & \sin\phi/\cos\theta & \cos\phi/\cos\theta \end{pmatrix} \begin{pmatrix} p \\ q \\ r \end{pmatrix}, \tag{3}$$

where ϕ, θ, ψ are the roll, pitch, and yaw angles, respectively, and p, q, r are the roll, pitch, and yaw rates, respectively. Lastly, the rotation dynamics is given as

$$\dot{\omega} = J^{-1}(M - \omega \times J\omega), \tag{4}$$

where $\omega = (p \;\; q \;\; r)^T$ is the angular rate and J is the inertia matrix.

C. Decoupled Vertical and Lateral Dynamics

The control algorithm decouples the dynamics into heave and lateral dynamics. The heave dynamics describes the ship deck heave motion, and the vertical controller maintains the relative vertical position between the quadrotor and the ship deck. Fig. 1 shows a block diagram of the overall control structure.

The thrust vector in the inertial reference frame is

$$\begin{aligned} T^{(i)} &= -R_{bi}^T T\hat{e}_3 \\ &= -\begin{pmatrix} \sin\phi\sin\psi + \cos\phi\sin\theta\cos\psi \\ -\sin\phi\cos\psi + \cos\phi\sin\theta\sin\psi \\ \cos\phi\cos\theta \end{pmatrix} T. \end{aligned} \tag{5}$$

The z component of (2) can be rewritten as

$$m\ddot{h} = T\cos\phi\cos\theta - mg, \tag{6}$$

where $h = -z$ is the height of the quadrotor. It is also noted that wind disturbance is relatively significant in the open sea environment; therefore, this approach also considers the impact of wind disturbance. In this case, (6) becomes

$$m\ddot{h} = T\cos\phi\cos\theta - mg + md_w, \tag{7}$$

where d_w is the acceleration due to wind disturbance.

Letting $h_1 = h$, $h_2 = \dot{h}_1$, and $u = \frac{T}{m}\cos\phi\cos\theta - g$, (6) can be rewritten as

$$\dot{h}_1 = h_2, \tag{8a}$$

$$\dot{h}_2 = u + d_w. \tag{8b}$$

In this case, the heave dynamics is decoupled from the planar dynamics using control transformation $T = \frac{mu+mg}{\cos\phi\cos\theta}$. It is further noted that T is limited by mechanical bounds, hence, the virtual control u is also limited.

In this problem, the quadrotor is required to track the heave motion of the ship deck d_s. The tracking error is given by $e_1 = h_1 - d_s - H$, where $H > 0$ is the commanded height above the ship deck. The tracking error dynamics becomes

$$\dot{e}_1 = e_2, \tag{9a}$$

$$\dot{e}_2 = u - \ddot{d}_s - \ddot{H} + d_w = u_{eq} - \ddot{d}_s + d_w, \tag{9b}$$

where $u_{eq} \triangleq u - \ddot{H}$. This can be further expressed as

$$\dot{e} = Ae + Bu_{eq} + D_1 w_s + D_2 w_d, \tag{10}$$

where $e = \left(\begin{smallmatrix} e_1 \\ e_2 \end{smallmatrix}\right)$, $A = \left(\begin{smallmatrix} 0 & 1 \\ 0 & 0 \end{smallmatrix}\right)$, $B = \left(\begin{smallmatrix} 0 \\ 1 \end{smallmatrix}\right)$, $D_1 = -\left(\begin{smallmatrix} 0 \\ \Delta_1 \end{smallmatrix}\right)$, $D_2 = \left(\begin{smallmatrix} 0 \\ \Delta_2 \end{smallmatrix}\right)$ are the system matrices and $\Delta_1 w_s = \ddot{d}_s$, $\Delta_2 w_d = d_w$ for all w_s and w_d such that $\|w_s\|_\infty = 1$ and $\|w_d\|_\infty = 1$. The parameters Δ_1 and Δ_2 can be estimated from the historical data of the ship deck heave motion at various sea states. The L_∞ signal norm is defined as $\|x\|_\infty = \sup_t \|x(t)\|_2$ for all time $t \geq 0$, and $\|x(t)\|_2$ is the Euclidean norm at time t.

REMARK 1 For lateral motion control, a lateral controller acts as a stabilizer to maintain the lateral position of the quadrotor above the landing platform. The control law is formulated using a backstepping technique. The equations of motion (1)–(4), are transformed into the strict feedback form for the application of the backstepping technique by considering the jerk dynamics. Interested readers can refer to [26, 27] for more details.

III. VERTICAL CONTROLLER

A. Invariant Ellipsoid Technique

The ship heave motion is relatively slow, evident from its low frequency, as compared to the response of the quadrotor. Therefore, the quadrotor is able to reasonably compensate for the ship heave motion up to within a certain error bound. This error bound arises from the finite time delay between feedback and compensation. However, a sufficiently high gain feedback can lower this bound. The following analysis, an expansion of the approach proposed by Nazin et al. [19], determines appropriate feedback gain with an estimation of the error bound and consideration of the control limits in the presence of multiple disturbances. Interested reader can refer to [19, 20].

Consider a feedback control of the form

$$u_{eq} = Ke, \tag{11}$$

where K is the feedback gain, and (10) becomes

$$\dot{e} = (A + BK)e + D_1 w_s + D_2 w_d. \tag{12}$$

Now consider a Lyapunov function of the form

$$V = e^T Qe, \tag{13}$$

where $Q = Q^T > 0$ is to be determined. Its derivative is

$$\dot{V} = e^T (QA + QBK + (*))e + 2w_s^T D_1^T Qe + 2w_d^T D_2^T Qe, \tag{14}$$

where $X + (*) \triangleq X + X^T$ for any square matrix X.

For the response of the system to remain within an ellipsoid given by $V \le 1$, the following condition must be satisfied, $e^T(QA + QBK + (*))e + 2w_s^T D_1^T Qe + 2w_d^T D_2^T Qe \le 0$ for all e, w_s, and w_d that satisfy $e^T Qe \ge 1$, $w_s^T w_s \le 1$, and $w_d^T w_d \le 1$ for all $t \ge 0$. This ellipsoid is known as the invariant ellipsoid in the sense that once the state enters the ellipsoid, it will remain within the ellipsoid.

Rewrite (14) as

$$x^T \begin{pmatrix} QA + QBK + (*) & QD_1 & QD_2 \\ D_1^T Q & 0 & 0 \\ D_2^T Q & 0 & 0 \end{pmatrix} x \le 0, \tag{15}$$

for all x where $x = (e \;\; w_s \;\; w_d)^T$ and satisfies

$$x^T \begin{pmatrix} -Q & 0 & 0 \\ 0 & 0 & 0 \\ 0 & 0 & 0 \end{pmatrix} x \le -1, \tag{16}$$

$$x^T \begin{pmatrix} 0 & 0 & 0 \\ 0 & I & 0 \\ 0 & 0 & 0 \end{pmatrix} x \le 1, \tag{17}$$

$$x^T \begin{pmatrix} 0 & 0 & 0 \\ 0 & 0 & 0 \\ 0 & 0 & I \end{pmatrix} x \le 1, \tag{18}$$

with I being the identity matrix. An execution of the S-procedure will reduce the conditions given by (15)–(18) to

$$\begin{pmatrix} QA + QBK + (*) + \tau_1 Q & QD_1 & QD_2 \\ D_1^T Q & -\tau_2 I & 0 \\ D_2^T Q & 0 & -\tau_3 I \end{pmatrix} \le 0, \tag{19}$$

for some $\tau_1 \ge \tau_2 + \tau_3$, $\tau_2 \ge 0$, and $\tau_3 \ge 0$.

Applying the Schur formula to (19), we get

$$QA + QBK + (*) + \tau_1 Q + \frac{1}{\tau_2} QD_1 D_1^T Q + \frac{1}{\tau_3} QD_2 D_2^T Q \le 0. \tag{20}$$

Letting $P = Q^{-1}$ and pre- and postmultiplying (20) by P yields

$$AP + BKP + (*) + \tau_1 P + \frac{1}{\tau_2} D_1 D_1^T + \frac{1}{\tau_3} D_2 D_2^T \le 0. \tag{21}$$

Observe that because $P > 0$, (21) can be reexpressed as

$$AP + BKP + (*) + (\tau_2 + \tau_3)P + \frac{1}{\tau_2} D_1 D_1^T + \frac{1}{\tau_3} D_2 D_2^T + (\tau_1 - \tau_2 - \tau_3)P \le 0, \tag{22}$$

where $\tau_1 - \tau_2 - \tau_3 \ge 0$. Therefore, a sufficient condition for $P > 0$ to be an invariant ellipsoid is

$$PA^T + AP + BKP + PK^T B^T + (\tau_2 + \tau_3)P + \frac{1}{\tau_2} D_1 D_1^T + \frac{1}{\tau_3} D_2 D_2^T \le 0. \tag{23}$$

All invariant ellipsoids, including the minimum invariant ellipsoid, satisfy this condition.

If (23) is satisfied, then the response will be bounded within an ellipsoid given by $e^T P^{-1} e \le 1$. Let $Y = KP$, then (23) is linear in variables P and Y.

$$PA^T + AP + BY + Y^T B^T + (\tau_2 + \tau_3)P + \frac{1}{\tau_2} D_1 D_1^T + \frac{1}{\tau_3} D_2 D_2^T \le 0. \tag{24}$$

Furthermore, it is reasonable to restrict the control action within the invariant ellipsoid. This can be done by considering $\|u(t)\|_R^2 = \|Ke(t)\|_R^2 \le u_{\max}^2$ at all time t, defined as $e^T K^T RKe \le u_{\max}^2$, where $R = R^T > 0$ is an invertible scaling matrix. This condition is to be satisfied for all $e^T Qe \le 1$. By performing the S-procedure, this condition is reduced to

$$K^T RK \le \tau Q, \tag{25}$$

for $\tau \le u_{\max}^2$.

Because the minimal ellipsoid is of interest, we set $\tau = u_{\max}^2$, pre- and postmultiply by P, and use the relation $Y = KP$ to get

$$Y^T RY \le u_{\max}^2 P. \tag{26}$$

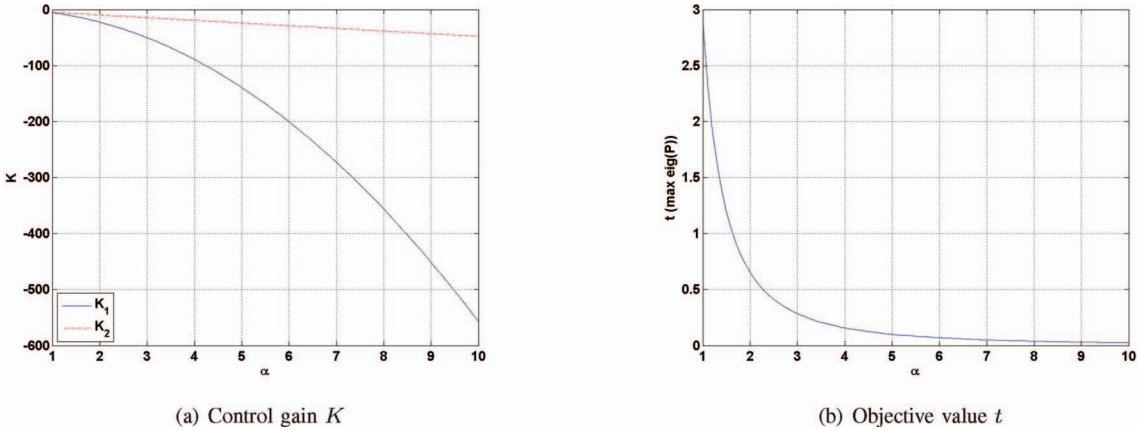

(a) Control gain K (b) Objective value t

Fig. 2. Variation of control gain K and maximum eigenvalue of P, i.e., $\lambda_1(P)$, with different values of α.

Applying of the Schur formula yields

$$\begin{pmatrix} P & Y^T \\ Y & u_{\max}^2 R^{-1} \end{pmatrix} \geq 0. \tag{27}$$

Therefore if (27) is satisfied, $\|u(t)\|_R^2 = \|Ke(t)\|_R^2 \leq u_{\max}^2$ for all $e^T Qe \leq 1$ and all $t \geq 0$. In typical cases, $R = I$ is imposed where I is an identity matrix.

From the discussion thus far, we are able to formulate a minimization problem to obtain the optimal gain K such that the invariant ellipsoid is minimized. Let the eigenvalues of P be $\lambda_1 \geq \lambda_2 \geq \cdots \geq \lambda_n > 0$. Then the eigenvalues of P^{-1} are $0 < \frac{1}{\lambda_1} \leq \frac{1}{\lambda_2} \leq \cdots \leq \frac{1}{\lambda_n}$. So $\frac{1}{\lambda_1}\|e\|_2 \leq e^T P^{-1} e \leq 1$ and $\|e\|_2 \leq \lambda_1$. Therefore the maximum eigenvalue of P is chosen as the objective function to be minimized.

The optimization problem is thus stated as follows:

$$\underset{P,Y,t}{\text{minimize}} \ t$$

subject to (24) and (27), $\tau_2 > 0$, $\tau_3 > 0$, and

$$P - tI \leq 0,$$
$$P \geq 0,$$

where I is an identity matrix. This optimization problem is a standard semidefinite programming problem and can be solved using many solvers such as *Yalmip*. The optimal control gain is obtained using the relation $K = YP^{-1}$.

This approach allows the computation of an optimal control gain K such that the invariant ellipsoid bound that is the performance measure is the smallest in the presence of unknown bounded disturbances. The key result in this approach is the extension of the invariant ellipsoid method presented in [15, 17] to allow analysis of multiple uncorrelated disturbances.

It is noted that the parameters τ_2 and τ_3 are to be defined independently. At different values of τ_2 and τ_3, different control gain $K = (K_1 \ K_2)$ and invariant ellipsoid P are obtained. A simple numerical simulation with $\tau_2 = \tau_3 = \alpha$ yields the variation of the control gains K_1 and K_2 in Fig. 2a and $t > \lambda_1(P)$ in Fig. 2b with varying α, where $\lambda_1(P)$ denotes the maximum eigenvalue of P. Fig. 2b shows that a higher α value is required to achieve a smaller ellipsoid, however, at the expense of a higher gain as shown in Fig. 2a. A proper choice of α is chosen to achieve a reasonable gain and invariant ellipsoid.

The controller derived using the invariant ellipsoid method exhibits other desirable properties. These include exponential convergence to the ellipsoid, preserved optimality for disturbance bounded by a value other than 1, and extension to stochastic disturbance.

1) *Preserved Optimality*: The optimality of the derived controller is preserved when the system is subjected to disturbance of a larger (smaller) bound. This is under the assumption that the maximum control action is enlarged (reduced) accordingly.

Suppose that the disturbance matrices D_1 and D_2 becomes $D_1' = \sqrt{\gamma} D_1$ and $D_2' = \sqrt{\gamma} D_2$, where $\gamma > 0$. The following transformation will transform the new optimization problem into the former problem: $P' = \gamma P$, $Y' = KP' = \gamma Y$, and $u'_{\max} = \sqrt{\gamma} u_{\max}$. So the resultant optimization becomes identical to the optimization problem with the original D_1 and D_2.

Therefore, the optimization of a controller subjected to a disturbance $\|w\|_\infty = \sqrt{\gamma}$ results in the same controller as before but with an invariant ellipsoid that is γ times the original size. This further implies that the invariant ellipsoids of different sizes form the level sets for different sizes of disturbance. Fig. 3 shows an illustration of the various invariant ellipsoid with the corresponding disturbance bound.

The key observation is that the same optimal control gain is obtained for disturbances that are enlarged or reduced correspondingly. The main difference is a mere scaling of the invariant ellipsoid. This observation is important for the analysis of stochastic disturbance.

2) *Exponential Attraction to Ellipsoid*: It is given in [20] that the time for an initial state e_0 with $e_0^T P^{-1} e_0 > \sigma$, $\sigma > 1$ to enter the invariant ellipsoid $e^T P^{-1} e < \sigma$ is

$$T_{\sigma,P} \leq \frac{1}{\alpha} \ln \frac{e_0^T P^{-1} e_0 - 1}{\sigma - 1}. \tag{28}$$

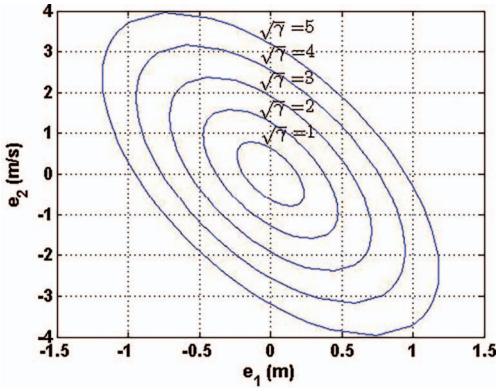

Fig. 3. Illustration of level set of error response bound when subjected to different levels of disturbance.

It is a common practice to let σ be a value slightly greater than 1, for instance, $\sigma = 1.05$.

This implies that if there is a sufficiently long period of time, $t \in [T_1, T_2]$ and $T_2 - T_1 > T_\gamma$,

$$T_{\sigma,\gamma P} = \frac{1}{\alpha} \ln \frac{\frac{1}{\gamma} e_0^T P^{-1} e_0 - 1}{\sigma - 1}, \tag{29}$$

for σ slightly greater than 1 such that the external disturbance bounds can be rewritten as $D_1' = \sqrt{\gamma} D_1$ and $D_2' = \sqrt{\gamma} D_2$ for $\gamma < 1$ (the disturbance is smaller than the designed value), then the error is expected to converge exponentially to a smaller ellipsoid given by $P' = \gamma P$. This is useful for the analysis of stochastic disturbance.

3) *Stochastic Disturbance*: A stochastic disturbance is a disturbance that takes the value according to a probability distribution. Disturbance is usually classified as a Gaussian disturbance and is characterized by its mean and variance. For a system subjected to stochastic disturbance, a controller that gives a minimal invariant ellipsoid also gives good stochastic disturbance rejection.

This is because the level set for each level of ellipsoid γP for $\gamma > 0$ is a minimum ellipsoid for disturbance $\|w\|_2 \leq \sqrt{\gamma}$. Furthermore if $\|w\|_2 \leq \sqrt{\gamma}$, then for $t > T_{\sigma,\gamma P}$, the state is guaranteed to converge into the ellipsoid γP. For a given disturbance generated by a stochastic process, the control gains obtained from the invariant ellipsoid method ensures that the state remains in the minimum possible ellipsoid $\gamma_{\min} P$ where $\gamma_{\min} = \inf \|w(t)\|_2$ for any time period $t_1 \leq t \leq t_2$ satisfying $t_2 - t_1 \geq T_{\sigma,\gamma_{\min} P}$. In other words, a randomly chosen time period will result in the state converging to the minimum possible ellipsoid. These properties are examined in Section IV.

B. Measurement Noises

It can be seen that the ship deck motion is modeled as a form of output disturbance in this formulation. The invariant ellipsoid method is used to obtain an optimal gain that results in a response that is bounded in a minimum ellipsoid.

In the case of input disturbance such as measurement noise, the impact to the system response is more intricate. We assume that the state measurement is subjected to noise n and the measured state becomes $\bar{e} = e + n$. This is fed back into the quadrotor system using a state feedback controller $u_{eq} = K\bar{e}$.

Therefore the effect of input disturbance becomes amplified with a high gain design. On the other hand, Fig. 2 suggests that a high gain design is necessary for a small invariant ellipsoid.

This constitutes a trade-off between a high gain design that results in the reduction of the effect of output disturbance (ship deck motion) and a low gain that results in lower sensitivity to input disturbances (measurement noise and wind disturbance). An optimal gain that balances these effects is desired.

In its analysis, the closed-loop system becomes

$$\dot{e} = (A + BK)e + BKn + D_1 w_s + D_2 w_d. \tag{30}$$

We assume the input disturbance is uncorrelated and bounded such that $n = Ew_n$, where E is a diagonal matrix containing the maximum bound information and $\|w_n\|_\infty = 1$.

It is clear that a closed-loop system in (30) will result in an optimization problem that is nonlinear because of the K in the term $BKn = BKEw_n$. Therefore, another approach is used to obtain the control gain K.

The control gain for an initial range of α is computed without the consideration of input disturbance. Due to input disturbance, the invariant ellipsoid under the computed gain K will be expanded. This expansion is found by obtaining the minimum invariant ellipsoid among the solution of the following optimization problem for a range of α. The optimization problem is

$$\underset{P,t}{\text{minimize}} \ t$$

subject to

$$\begin{gathered} P(A + BK)^T + (A + BK)P + (\tau_2 + \tau_3 + \tau_4)P \\ + \tfrac{1}{\tau_2} D_1 D_1^T + \tfrac{1}{\tau_3} D_2 D_2^T + \tfrac{1}{\tau_4} (BKE)(BKE)^T \leq 0, \\ P - tI \leq 0, \\ P \geq 0. \end{gathered}$$

An evaluation of the expansion in invariant ellipsoid with $\tau_2 = \tau_3 = \tau_4 = \alpha$ is performed and shown in Fig. 4. It is seen that the size of the invariant ellipsoid after considering input disturbance is significantly larger than the size before noise is added for all values of α and also becomes increasingly larger after a critical α (size). This shows that there is a limit to the minimum size of the invariant ellipsoid given a specific input disturbance. This critical size provides the critical control gain K that gives the best performance in the presence of input and output disturbances.

It is noted that input disturbance such as measurement noise is commonly modeled stochastically. However, from previous discussion, this approach can be extended to include stochastic disturbance.

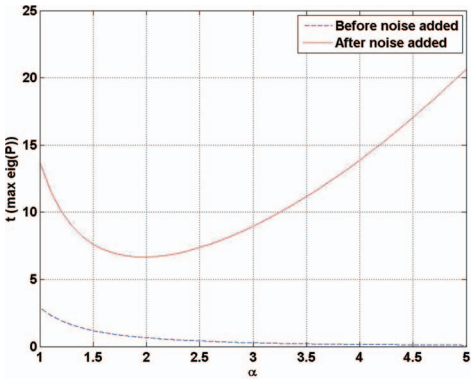

Fig. 4. Variation of maximum eigenvalue of invariant ellipsoid with α before and after introduction of noise.

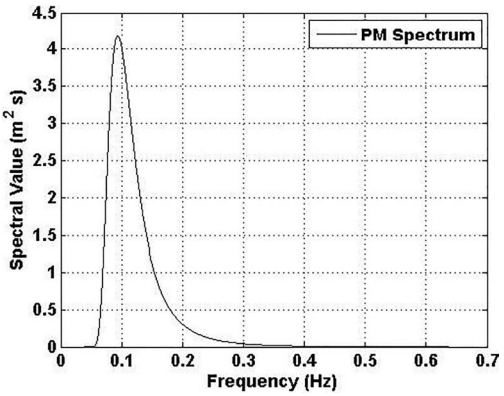

Fig. 5. Modified PM spectrum at sea state 6 and constant wind speed of 30 kt.

IV. NUMERICAL SIMULATION

We implement the control algorithm numerically using Matlab. In this section, the ship deck heave model used in the simulation is first described followed by the results and discussion.

A. Ship Deck Heave Model

The ship deck is assumed to exhibit heave motion from the interaction with the sea wave motion. A ship with a unity response amplitude operator is assumed without any loss of generality.

A sea wave model is derived using the energy spectrum and the ship deck is assumed to perform only heave motion in sync with the wave. The sea wave elevation is approximated into a Fourier series consisting of sinusoidal waves at different energy content (amplitude), frequency, and phase [29, 30].

The energy content at a particular sea state depends on the wave height spectrum. The modified Pierson-Moskowitz (PM) spectrum is used in this simulation. The modified PM spectrum is

$$S(\omega) = H_{1/3}^2 T_1 \frac{0.11}{2\pi}\left(\frac{\omega T_1}{2\pi}\right)^{-5} \exp\left[-0.44\left(\frac{\omega T_1}{2\pi}\right)^{-4}\right], \tag{31}$$

where $S(\omega)$ is the wave height spectrum, $H_{1/3}$ is the significant wave height, T_1 is the mean wave period, and ω is the frequency. $H_{1/3}$ and T_1 are dependent on the steady wind speed and sea state. Fig. 5 shows the modified PM spectrum generated for sea state 6 at a constant wind speed of 30 kt.

Based on the wave height spectrum, a discretization can be performed to obtain a time series for the wave elevation:

$$d = \sum_{j=1}^{N} \sqrt{2S(\omega_j)\Delta\omega_j}\,\sin(\omega_j t + \epsilon_j), \tag{32}$$

where d is the wave elevation, N is the number of waves to be modelled, $\Delta\omega_j$ is the discretization interval, and ω_j and ϵ_j are the frequency and phase of the jth wave, respectively. ϵ_j is determined from the initial state of the wave and is randomly assigned in the simulation. The time series of the wave elevation is simulated for two different initial conditions at sea state 6 and a constant wind speed of 30 kt and is shown in Fig. 6 to highlight the pseudorandomness of the wave elevation at a discretization of $N = 500$.

B. Simulation

A full nonlinear numerical simulation is performed on a generic quadrotor using parameters obtained from [31]. The parameters are listed in Table I. The invariant ellipsoid controller of Section III is used to control the heave motion, while the backstepping controller of [26] is used to control the lateral motion.

The quadrotor is initially placed at a 10 m height above the mean sea level and is displaced 1 m away in the planar directions from the intended landing pad, i.e., $(x_0 \;\; y_0 \;\; z_0)^T = (1 \;\; 1 \;\; -10)^T$. The landing pad is located on the ship deck, which is at 1 m above the sea level. The controller is commanded to bring and maintain the quadrotor at a spot 10 m above the landing location for 50 s. In this phase, the quadrotor attempts to follow the ship deck heave motion while limiting the relative motion error to within the invariant ellipsoid. Thereafter, the height of the quadrotor is reduced gradually in the landing phase. A smooth sigmoid function is chosen as the reference path,

$$H = H_0 + \frac{(H_f - H_0)}{1 + \exp\left(\frac{-6(2(t-t_0)-\Delta t)}{\Delta t}\right)}, \tag{33}$$

where H_0 and H_f are the initial and final height, respectively, t_0 is the time when the height is commanded to decrease, and Δt is the time duration of the descent. In this simulation, the following parameters are used. $H_0 = 10$, $H_f = 1$, $t_0 = 50$, and $\Delta t = 30$.

Measurement noises are added to the system as Gaussian white noise acting on the relative vertical position and vertical velocity measurements. The measurement noise is given by $n = Ew_n$ where $E = \text{diag}(0.141, 0.141)$ and $\|w_n\|_\infty = 1$. Furthermore, measurement noises are also added as Gaussian white

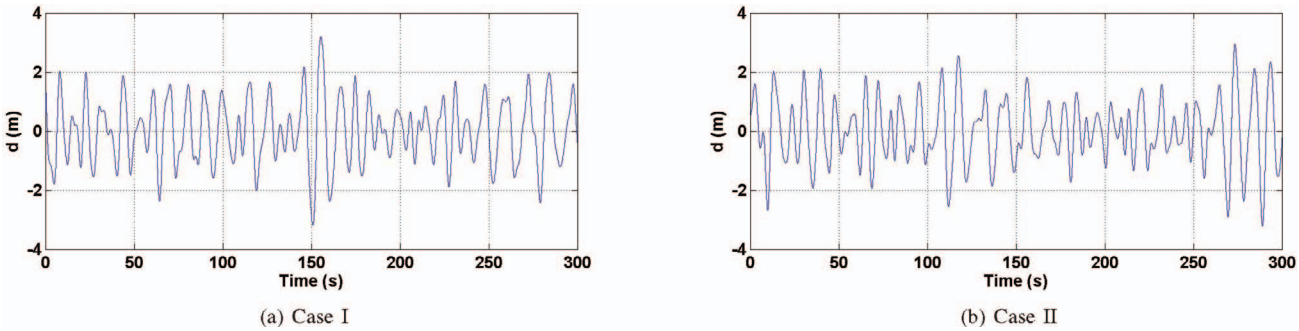

Fig. 6. Simulation of ship deck motion at sea state 6 at constant wind speed of 30 kt for two different initial conditions. Simulation shows that different waveforms are obtained by differing initial conditions.

TABLE I
A List of Quadrotor Parameters Used in the Simulation [31]

Parameters	Values
Mass (m)	1.25 kg
Distance between the rotor and center (l)	0.5 m
Moment of inertia to x-axis (J_{xx})	8.1×10^{-3} Nms^{-2}
Moment of inertia to y-axis (J_{yy})	8.1×10^{-3} Nms^{-2}
Moment of inertia to z-axis (J_{zz})	14.2×10^{-3} Nms^{-2}
Lift factor k_l	54.2×10^{-6} Ns^2
Drag factor k_d	1.1×10^{-6} Ns^2

noise to the planar states measurements to simulate the effect of measurement noise as well as lateral ship movement.

In addition, the effect of wind disturbance is also included in this simulation. Wind disturbance acting on the quadrotor exerts an aerodynamic force that affects the translational dynamics. The translational dynamics in (2) is altered as

$$m\dot{v}^{(i)} = -R_{bi}^T T\hat{e}_3 + mg\hat{e}_3 - K_w V_{\text{wind}}, \tag{34}$$

where the term $K_w V_{\text{wind}}$ is added to represents the aerodynamic force generated by the wind V_{wind}, and $K_w > 0$ is the aerodynamic force coefficient. The wind consists of a constant component as well as a random component and serves to realistically simulate the windy environment in the open seas. This is written as

$$V_{\text{wind}} = V_{\text{const}} + V_{\text{rand}}, \tag{35}$$

where V_{rand} is the random component bounded by $\|V_{\text{rand}}\|_\infty < 0.5$ m/s in this simulation and V_{const} is the constant component corresponding to an expected wind speed of 30 kt = 15.4 m/s at sea state 6.

The control parameters are generated by solving the optimization problem with $\alpha = 2.0$ using the controller of the form $u_{eq} = Ke$. This α value results in control gains $K_1 = -22.3$ and $K_2 = -9.5$ that gives rise to a minimum ellipsoid $V = e^T P_1 e = 1$ where $P_1 = \left(\begin{smallmatrix} 0.0558 & -0.1117 \\ -0.1117 & 0.6316 \end{smallmatrix}\right)$ and a global minimum invariant ellipsoid $V = e^T P_2 e = 1$ where $P_2 = \left(\begin{smallmatrix} 0.5296 & -1.5888 \\ -1.5888 & 6.2453 \end{smallmatrix}\right)$ after measurement noises are considered. The ellipsoids are shown in Fig. 7.

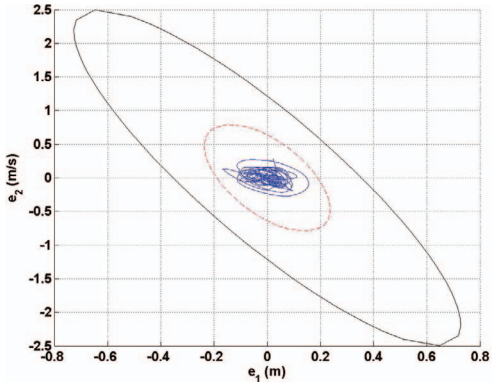

Fig. 7. Phase diagram of state e and invariant ellipsoid $V = e^T P_1 e = 1$ (red dotted line). Also shown is invariant ellipsoid after considering influence of measurement noise $V = e^T P_2 e = 1$ (black solid line). State of system is shown to be bounded within invariant ellipsoid $V = e^T P_2 e \leq 1$ after including effects of measurement noise.

The planar control gains used in this simulation are $K_1^{(\text{planar})} = K_2^{(\text{planar})} = \text{diag}(1,1)$ and $K_3^{(\text{planar})} = K_4^{(\text{planar})} = \text{diag}(3,3,3)$. Because the focus of this paper is the landing of the quadrotor, it is sufficient to show that the planar controller shown is able to maintain the position of the quadrotor above a fixed point over the ship. The simulation results are shown in Figs. 7–9.

C. Discussion

The simulation result shows that the proposed control algorithm is able to track the ship deck motion in the presence of measurement noise to within a good performance bound, thus being able to land on a ship heaving in the open sea at sea state 6. More importantly, the simulation shows that the invariant ellipsoid method is able to synthesize control gains that result in good performance. Furthermore, the lateral control also performed well under the coupling from the heave/altitude controller.

Fig. 7 shows the phase diagram of the states e_1 and e_2 with the invariant ellipsoid $V = 1$. It shows both the invariant ellipsoid with and without consideration of measurement noises. The larger ellipsoid is computed with measurement noises and, hence, is the representative ellipsoid in this

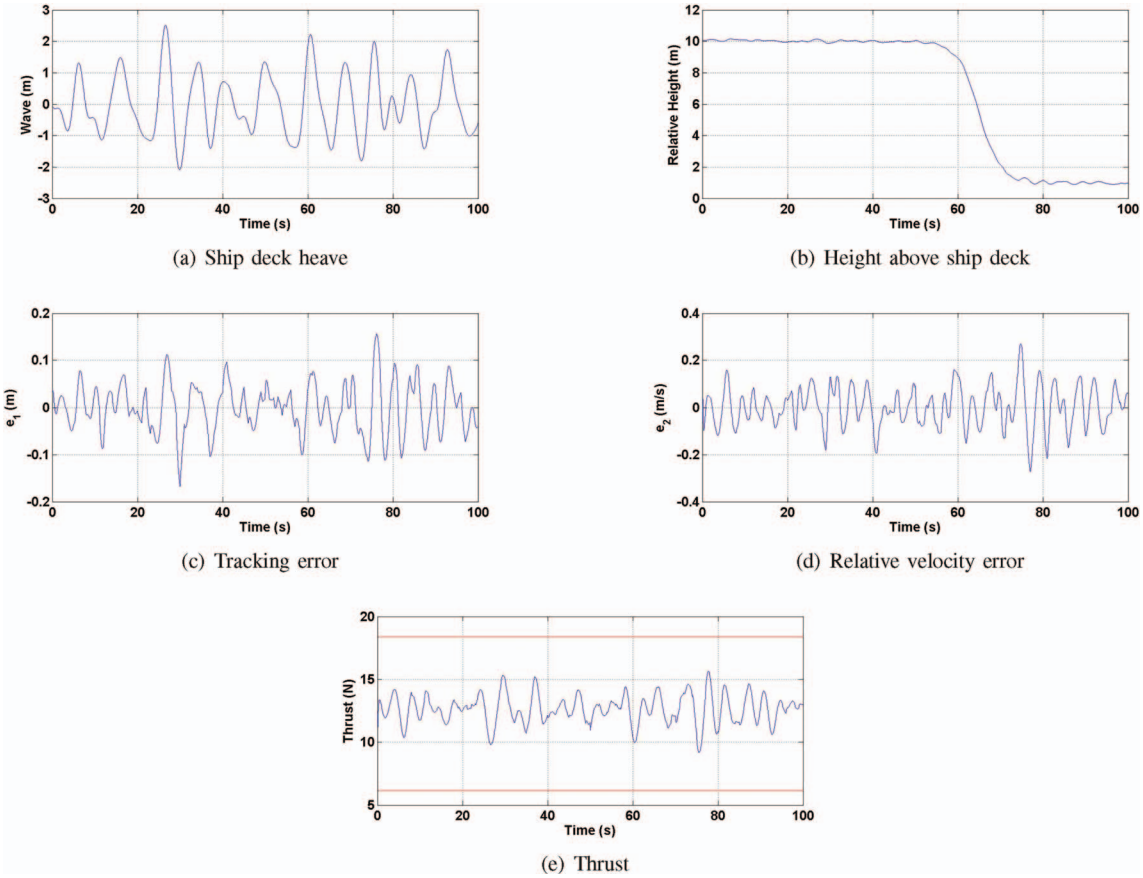

Fig. 8. Simulation results of quadrotor landing on ship deck showing vertical parameters. (a) Heave motion of ship deck, with mean sea level at $d = 0$; (b) height of quadrotor relative to ship deck and landing pad is located at 1 m above ship deck; (c) tracking error e_1 of quadrotor, where small tracking error indicates that quadrotor is able to track ship deck motion; (d) in contrast, relative velocity error with ship deck, where small value indicates small impact velocity; and (e) thrust input of quadrotor and limits.

simulation. The states were initially outside the ellipsoid and is attracted to the ellipsoid and remains within it thereafter. The states are guaranteed to remain in the Lyapunov level set $V \leq 1$ by the formulation of the problem.

Fig. 8c shows the tracking error of the quadrotor. The error remains sufficiently small for practical application on ship deck landing. Furthermore, Fig. 8b shows the height of the quadrotor above the ship deck. Smooth and safe landing is achieved in this simulation. More importantly, the impact upon landing depends on the relative velocity between the ship and the quadrotor, which is measured by e_2, Fig. 8d shows that the relative velocity remains sufficiently small such that the impulse upon landing (0.3 Ns in the simulation) is practically small. Furthermore, the invariant ellipsoid information given in Fig. 7 shows that the change in momentum upon landing is at most approximately 3 Ns.

In addition, the planar control performs adequately to maintain the quadrotor above the landing platform in the presence of lateral ship motion and measurement noises (see Fig. 9). Furthermore the constant wind induces an average pitch angle of 15°, nevertheless it does not impact the vertical control since the motions are decoupled using control transformation $T = \frac{mu+mg}{\cos\phi\cos\theta}$. Because the focus of this paper is on the landing of the quadrotor, it suffices to show the adequacy of the planar controller.

D. Response to Stochastic Disturbance

It is also common to model the ship deck motion as a form of stochastic disturbance. A numerical simulation is performed with the disturbance w modeled as a stochastic variable that has the probability to exceed the design limit of $\|w\|_2 = 1$. The quadrotor is placed at an initial height $h = 10$ m and is required to maintain a relative height of 10 m. The results are shown in Figs. 10 and 11.

An instance of small disturbance is extracted to highlight the reduction of the ellipsoid during the time frame when the disturbance is small. The results are shown in Figs. 12 and 13.

It is clear that the proposed controller is able to handle stochastic disturbance very well as seen from its ability to restrict the states to the ellipsoid characterized by the maximum disturbance (see Fig. 10). During instances where the disturbance is smaller, the states are bounded by a smaller ellipsoid characterized by the maximum disturbance during that period of time (see Fig. 12). In stochastic disturbance, large values only occur for a brief period of time; therefore, the states' response is often

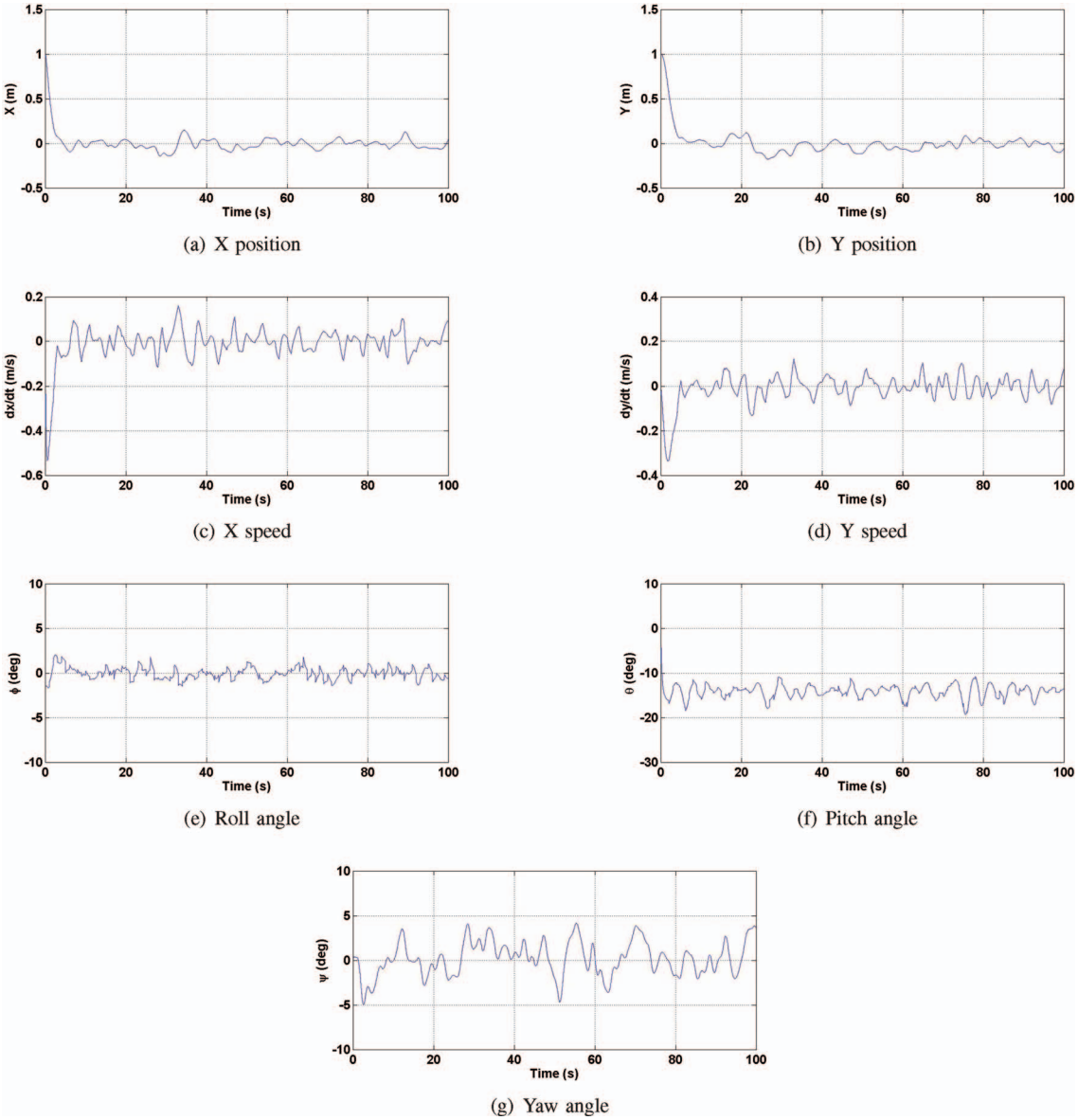

Fig. 9. Simulation results of quadrotor landing on ship deck showing lateral parameters. (a) and (b) X and Y position, respectively, of quadrotor and ability to move to (0, 0) from (1, 1); (c) and (d) speed of quadrotor in X and Y directions, respectively; and (e), (f), and (g) attitude of quadrotor during movement.

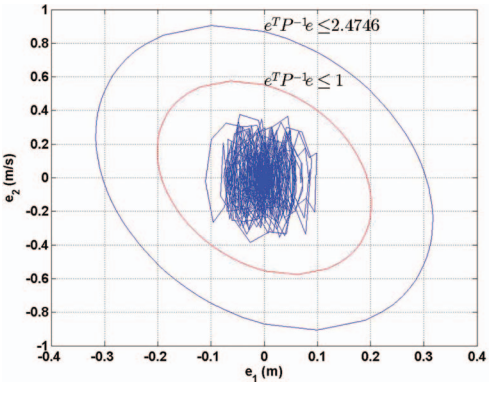

Fig. 10. Phase diagram of state e. Invariant ellipsoid $V = 1$ and ellipsoid based on maximum disturbance $V = 2.4746$ are shown. State of system bounded within invariant ellipsoid, $V \leq 2.4746$.

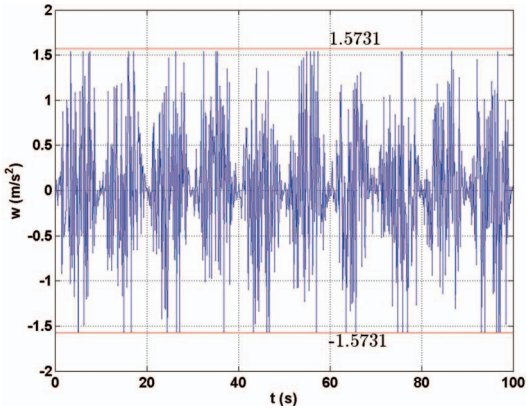

Fig. 11. Ship deck heave motion that is modeled as stochastic disturbance.

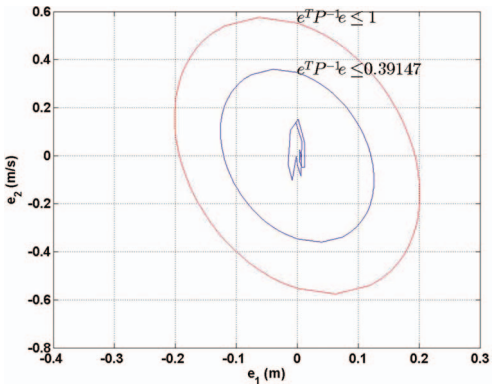

Fig. 12. Phase diagram of state e. Invariant ellipsoid $V = 1$ and ellipsoid based on maximum disturbance during time interval considered $V = 0.39147$ are shown. State of system bounded within invariant ellipsoid, $V \leq 0.39147$.

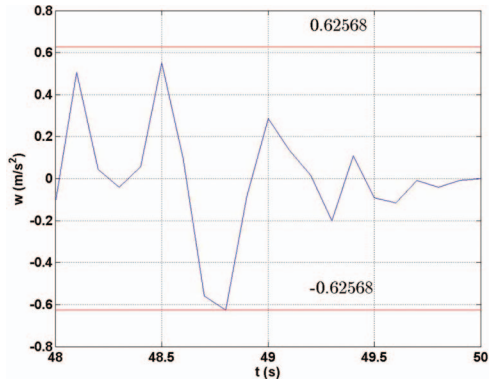

Fig. 13. Time frame of small disturbance where maximum disturbance during that time frame is shown.

bounded by a smaller ellipsoid as compared to the ellipsoid formed by the global maximum disturbance. Nevertheless, the same control gain yield the minimum ellipsoid for different levels of disturbances, and therefore it is effective against stochastic disturbance that has an occasional increase in disturbance values.

V. CONCLUSION

The problem of UAV landing on a ship deck subjected to nontrivial heave motion, wind disturbance, and measurement noise is solved using the invariant ellipsoid method on a quadrotor. Optimal state feedback gain is obtained using the invariant ellipsoid method for different α values corresponding to different optimal ellipsoid sizes. Measurement noise is shown to expand the invariant ellipsoid as the control gain increases and the α value that results in a minimum invariant ellipsoid under measurement noise is computed. In addition, a lateral motion controller was also synthesized using backstepping technique. The heave/altitude controller was able to achieve good landing performance in the presence of pseudorandom ship deck heave motion, wind disturbance, and measurement noise as verified by simulations. The ability of the heave/altitude controller to maintain constant relative height above the ship deck when the ship deck is modeled as a stochastic disturbance is also demonstrated.

REFERENCES

[1] Avanzini, G., Busato, A., and de Matteis, G.
Trajectory generation and tracking for ship deck landing of a VTOL vehicle.
Presented at the *AIAA Atmospheric Flight Mechanics Conference and Exhibit*, Montreal, Canada, 2001.

[2] Marconi, L., Isidori, A., and Serrani, A.
Autonomous vertical landing on an oscillating platform: An internal-model based approach.
Automatica, **38**, 1 (Jan. 2002), 21–32.

[3] Yang, X., Pota, H., Garratt, M., and Ugrinovskii, V.
Prediction of vertical motions for landing operations of UAVs.
In *2008 47th IEEE Conference on Decision and Control*, 2008, 5048–5053.

[4] Yang, X., Garratt, M., and Pota, H.
Monotonous trend estimation of deck displacement for automatic landing of rotorcraft UAVs.
Journal of Intelligent and Robotic Systems: Theory and Applications, **61** (2011), 267–285.

[5] Garratt, M., Pota, H., Lambert, A., Eckersley-Maslin, S., and Farabet, C.
Visual tracking and LIDAR relative positioning for automated launch and recovery of an unmanned rotorcraft from ships at sea.
Naval Engineers Journal, **121**, 2 (Jun. 2009), 99–110.

[6] Arora, S., Jain, S., Scherer, S., Nuske, S., Chamberlain, L., and Singh, S.
Infrastructure-free shipdeck tracking for autonomous landing.
In *2013 IEEE International Conference on Robotics and Automation*, May 2013, 323–330.

[7] Xu, G., Zhang, Y., Ji, S., Cheng, Y., and Tian, Y.
Research on computer vision-based for UAV autonomous landing on a ship.
Pattern Recognition Letters, **30**, 6 (Apr. 2009), 600–605.

[8] Herisse, B., Hamel, T., Mahony, R., and Russotto, F.-X.
Landing a VTOL unmanned aerial vehicle on a moving platform using optical flow.
IEEE Transactions on Robotics, **28**, 1 (Feb. 2012), 77–89.

[9] Sanchez-Lopez, J. L., Saripalli, S., Campoy, P., Pestana, J., and Fu, C.
Toward visual autonomous ship board landing of a VTOL UAV.
In *2013 International Conference on Unmanned Aircraft Systems (ICUAS)*, May 2013, 779–788.

[10] Yakimenko, O., Kaminer, I., Lentz, W., and Ghyzel, P.
Unmanned aircraft navigation for shipboard landing using infrared vision.
IEEE Transactions on Aerospace and Electronic Systems, **38**, 4 (Oct. 2002), 1181–1200.

[11] Venugopalan, T. K., Taher, T., and Barbastathis, G.
Autonomous landing of an unmanned aerial vehicle on an autonomous marine vehicle.
Presented at the *OCEANS 2012 MTS/IEEE: Harnessing the Power of the Ocean*, 2012.

[12] Ling, K., Chow, D., Das, A., and Waslander, S. L.
Autonomous maritime landings for low-cost VTOL aerial vehicles.
In *Proceedings of the Conference on Computer and Robot Vision, CRV 2014*, 2014, 32–39.

[13] Sandino, L. A., Bejar, M., and Ollero, A.
On the applicability of linear control techniques for autonomous landing of helicopters on the deck of a ship.
In *2011 IEEE International Conference on Mechatronics*, Apr. 2011, 363–368.

[14] Huh, S., and Shim, D. H.
A vision-based landing system for small unmanned aerial vehicles using an airbag.
Control Engineering Practice, **18**, 7 (Jul. 2010), 812–823.

[15] Tan, C. K., and Wang, J.
A novel PID controller gain tuning method for a quadrotor landing on a ship deck using the invariant ellipsoid technique.
In *2014 14th International Conference on Control, Automation and Systems (ICCAS 2014)*, 2014, 1339–1344.

[16] Ngo, T. D., and Sultan, C.
Nonlinear helicopter and ship models for predictive control of ship landing operations.
In *AIAA Guidance, Navigation, and Control Conference*, Jan. 2014, 1–19.

[17] Tan, C. K., and Wang, J.
Ship deck landing of a quadrotor using the invariant ellipsoid technique.
In *2014 Proceedings of the SICE Annual Conference (SICE)*, Hokkaido, Japan, 2014, 1443–1448.

[18] Chellaboina, V., Leonessa, A., and Haddad, W. M.
Generalized Lyapunov and invariant set theorems for nonlinear dynamical systems.
Systems & Control Letters, **38**, 4–5 (Dec. 1999), 289–295.

[19] Nazin, S. A., Polyak, B. T., and Topunov, M. V.
Rejection of bounded exogenous disturbances by the method of invariant ellipsoids.
Automation and Remote Control, **68**, 3 (Mar. 2007), 467–486.

[20] Khlebnikov, M. V., Polyak, B. T., and Kuntsevich, V. M.
Optimization of linear systems subject to bounded exogenous disturbances: The invariant ellipsoid technique.
Automation and Remote Control, **72**, 11 (Nov. 2011), 2227–2275.

[21] Gonzalez-Garcia, S., Polyakov, A., and Poznyak, A.
Linear feedback spacecraft stabilization using the method of invariant ellipsoids.
In *2009 41st Southeastern Symposium on System Theory*, Mar. 2009, 195–198.

[22] Polyakov, A., and Poznyak, A.
Invariant ellipsoid method for minimization of unmatched disturbances effects in sliding mode control.
Automatica, **47**, 7 (Jul. 2011), 1450–1454

[23] Gonzalez-Garcia, S., Polyakov, A., and Poznyak, A.
Output linear feedback for a class of nonlinear systems based on the invariant ellipsoid method.
In *2008 5th International Conference on Electrical Engineering, Computing Science and Automatic Control*, Nov. 2008, 7–12.

[24] Azhmyakov, V.
On the geometric aspects of the invariant ellipsoid method: Application to the robust control design.
In *IEEE Conference on Decision and Control and European Control Conference*, Dec. 2011, 1353–1358.

[25] Azhmyakov, V., Poznyak, A., and Juárez, R.
On the practical stability of control processes governed by implicit differential equations: The invariant ellipsoid based approach.
Journal of the Franklin Institute, **350**, 8 (Oct. 2013), 2229–2243.

[26] Tan, C. K., Wang, J., and Paw, Y. C.
Tracking of a moving ground target by a quadrotor using a backstepping approach based full state cascaded dynamics.
Applied Soft Computing. Submitted for publication, 2015.

[27] Tan, C. K.
Ship deck landing of multi-rotor unmanned aerial vehicle.
Ph.D. dissertation, Nanyang Technological University, Singapore, 2015.

[28] Stevens, B. L., and Lewis, F. L.
Aircraft Control and Simulation, 2nd ed. Hoboken, NJ: John Wiley and Sons, 2003.

[29] Tristan, P., and Blanke, M.
Simulation of ship motion in seaway.
Department of Electrical and Computer Engineering, The University of Newcastle, Australia, Tech. Rep. EE02037, 2002.

[30] Brekken, T. K. A., Ozkan-Haller, H. T., and Simmons, A.
A methodology for large-scale ocean wave power time-series generation.
IEEE Journal of Oceanic Engineering, **37**, 2 (Apr. 2012), 294–300.

[31] Gong, X., Bai, Y., Hou, Z., Zhao, C., Tian, Y., and Sun, Q.
Backstepping sliding mode tracking control of quad-rotor under input saturation.
International Journal of Intelligent Computing and Cybernetics, **5**, 4 (2012), 515–532.

Chun Kiat Tan received his B.Eng. degree in aerospace engineering from Nanyang Technological University, Singapore in 2011. He is currently pursuing his Ph.D. degree at the School of Mechanical and Aerospace Engineering, Nanyang Technological University, Singapore. His research interests include mathematical modeling, numerical simulation, control theory, flight dynamics, flight planning, unmanned systems and multiagent systems.

Jianliang Wang received the B.E. degree in electrical engineering from Beijing Institute of Technology, China, in 1982. He received the M.S.E. and Ph.D. degrees in electrical engineering from The Johns Hopkins University, MD, in 1985 and 1988, respectively, specializing in nonlinear systems and control theory.

From 1988 to 1990, he was a lecturer with the Department of Automatic Control at Beijing University of Aeronautics and Astronautics, China. Since 1990, he has been with the School of Electrical and Electronic Engineering at Nanyang Technological University, Singapore, where he is currently an associate professor. His research interest includes multiagent systems, vision-based control systems, robust and reliable control, path planning and trajectory generation, and flight control systems.

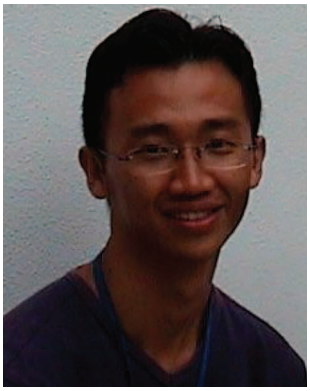

Yew Chai Paw received the B.Eng. and M.Eng. degrees in mechanical and aerospace engineering from Nanyang Technology University, Singapore, in 2000 and 2005, respectively. He received the Ph.D. degree in aerospace engineering in 2009 from University of Minnesota, MN. He is currently a principal member of technical staff in DSO National Laboratories, Singapore. His research interests include UAV system engineering and flight dynamics modeling.

Fang Liao received her B.E. and M.E. degrees in control and navigation, both from Beijing University of Aeronautics and Astronautics, China, in 1992 and 1995, respectively, and her Ph.D. degree from Nanyang Technological University, Singapore, in 2003. She was an engineer in the Research Institute of Unmanned Air Vehicles at Beijing University of Aeronautics and Astronautics from 1995 to 1999 and a research associate and then research fellow in the School of Electrical and Electronic Engineering at Nanyang Technological University from 2002 to 2004. Since 2004, she has been a research scientist in Temasek Laboratories at National University of Singapore. Her research interests include robust and adaptive control theories and application, fault tolerant control, cooperative control, multiagent systems, and constrained optimization methods.